Taylor, G. I., "The Criterion for Turbulence in Curved Pipes," *Proc. Royal Soc., Ser. A*, **124**, 243 (1929).
Truesdell, L. C. Jr., and R. J. Adler, "Numerical Treatment of Fully Developed Laminar Flow in Helically Coiled Tubes," *AIChE J.*, **16**, 1010 (1970).
White, C. M., "Stream-Line Flow Through Curved Pipes," *Proc. Royal Soc.*, **A123**, 645 (1929).
Young, D. M., "Iterative Methods for Solving Partial Differential Equations of Elliptic Type," *Trans. Am. Math. Soc.*, **76**, 92 (1954).

Supplementary material has been deposited as Document No. 02671 with the National Auxiliary Publications Service (NAPS), Microfiche Publications, 440 Park Ave. South, New York, NY 10016, and may be obtained for $1.50 for microfiche or $5.00 for photocopies.

Manuscript received May 8, 1974; revision received February 12 and accepted April 2, 1975.

Part II. Oscillating Helically Coiled Tubes

B. JOSEPH
and
R. J. ADLER

Chemical Engineering Department
Case Institute of Technology
Case Western Reserve University
Cleveland, Ohio 44106

The numerical method of Part I is extended to study periodic laminar flow in helically coiled tubes of square cross section oscillating sinusoidally about their helix axis. Depending on the relative strength of the wall velocity and the velocity of flow through the tube, one of three flow regimes occur. When the wall velocity is small, the computed results resemble these for a stationary helix. When the wall velocity dominates, the direction of the secondary flow is reversed. When the wall and flow velocities are comparable, the secondary flow pattern varies periodically in time and sometimes alternates in direction.

SCOPE

This part explores fluid flow in helically coiled tubes of square cross section oscillating about their helix axis. The fluid near the wall is dragged back and forth by wall motion. When the wall velocity is larger than the flow velocity, the fluid near the wall experiences larger centrifugal forces than the interior fluid and is thus thrown outward, away from the helix axis. Replacement fluid flows inward through the center of the cross section. The resulting twin counterrotating vortices resemble those found in secondary flow in stationary helically coiled tubes (see Part I), but the rotation is in the opposite direction. These wall motion induced secondary flows can be very strong.

Helically coiled tubes oscillating about their helix axis have been proposed by Bartlett and Drinker et al. (1969) as blood oxygenators. Experiments show high rates of oxygen transfer across tube walls made for semipermeable silicone membranes into blood. Cross-sectional mixing by strong secondary flows induced by the wall motion substantially eliminated mass transfer resistance within the blood. Moss (1971) attempted by correlate friction factors and mass transfer rates based on an approximate analysis. Another proposed application is an inertia type of pump (Fisher, 1959-1963). The authors of this paper believe there are additional potential applications such as continuous blenders, continuous polymerization reactors, and continuous centrifuges.

The objective of this study is to use numerical methods to survey the interaction of flow through helically coiled tubes caused by a constant pressure or constant flow driving force and the oscillation of the helically coiled tubes. The seven cases studied vary the flow for a constant radius of curvature and frequency of oscillation.

CONCLUSIONS AND SIGNIFICANCE

The computed solutions confirm that oscillating a helically coiled tube about its mandrel axis can induce strong secondary flows. Three flow regimes can be distinguished. When the maximum velocity of the oscillating tube wall is small compared to the velocity of flow through the tube, the effect of the oscillation is to reduce the strength of the secondary flow associated with flow through stationary helically coiled tubes. When the wall velocities are comparable to the flow velocity, the secondary flow varies periodically with time, sometimes changing direction during the oscillation. When the wall velocities are large compared to the flow velocity, there are two strong counterrotating vortices in the cross section, rotating opposite in direction to those observed in stationary helically coiled tubes.

Numerical methods are judged practical for calculating flow solutions for oscillating helically coiled tubes, at least over the range of variables studied in this work; solutions required three to four min. of computer time (Univac 1108).

The results reported here, together with prior studies of others, give a more detailed and systematic picture of fluid flow in oscillating helically coiled tubes than has been available heretofore. It is hoped that the additional background will encourage further investigations and uses of oscillating helically coiled tubes for process applications (see Scope).

Correspondence concerning this paper should be addressed to R. J. Adler.

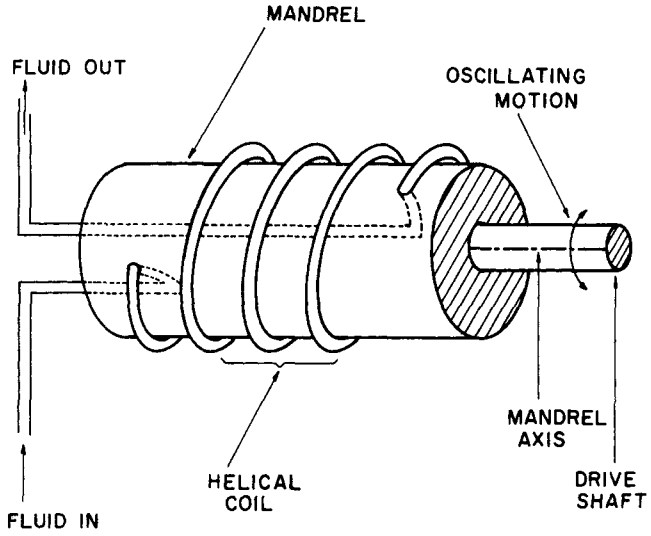

Fig. 1. Oscillating helix.

EQUATIONS OF MOTION

Consider a helix oscillating sinusoidally about its mandrel axis as shown in Figure 1. The angular velocity of the tube walls is a periodic function of time. For incompressible fluids the flow is fully developed except near the entrance and exit. As in Part I, the geometry of a torus is a good approximation for small angles of pitch. The coordinate system is the same as in Part I. The effect of the oscillation is to introduce a periodic boundary condition for axial velocity at the wall. The Navier-Stokes equations of motion and the continuity equations in dimensionless variables are as follows:

$$\frac{\partial U}{\partial T} = -U\frac{\partial U}{\partial X} - \frac{V}{\lambda}\frac{\partial U}{\partial Y} + \frac{(a/r)W^2}{1+(a/r)X} - \frac{\partial P}{\partial X} + \frac{1}{\lambda^2}\frac{\partial^2 U}{\partial Y^2} - \frac{1}{\lambda}\frac{\partial^2 V}{\partial X \partial Y} \quad (1a)$$

$$\frac{\partial V}{\partial T} = -U\frac{\partial V}{\partial X} - \frac{V}{\lambda}\frac{\partial V}{\lambda \partial Y} - \frac{1}{\lambda}\frac{\partial P}{\partial Y} + \frac{\partial^2 V}{\partial X^2} - \frac{1}{\lambda}\frac{\partial^2 U}{\partial X \partial Y} + \frac{(a/r)}{1+(a/r)X}\left[\frac{\partial V}{\partial X} - \frac{\partial U}{\partial Y}\right] \quad (1b)$$

$$\frac{\partial W}{\partial T} = -U\frac{\partial W}{\partial X} - \frac{V}{\lambda}\frac{\partial W}{\partial Y} - \frac{(a/r)UW}{1+(a/r)X} - \frac{1}{(1+(a/r)X)}\frac{\partial P}{\partial Z} + \frac{\partial^2 W}{\partial X^2} + \frac{1}{\lambda}\frac{\partial^2 W}{\partial Y^2} + \frac{(a/r)}{1+(a/r)X}\frac{\partial W}{\partial X} - \frac{(a/r)^2}{(1+(a/r)X)^2}W \quad (1c)$$

$$\frac{\partial}{\partial X}[1+(a/r)X]U + \frac{\partial}{\lambda \partial Y}[1+(a/r)X]V = 0 \quad (1d)$$

The flow is symmetric about the X-axis and hence a solution is necessary only in the upper half plane. Boundary conditions are based on no slip at the walls.

$$\left.\begin{aligned} U &= 0 \\ V &= 0 \\ W &= W_0[1+(a/r)X]\sin \Omega T \end{aligned}\right\} \text{along the wall boundary}$$

The factor $[1+(a/r)X]$ incorporates the effect of radius of curvature on the axial velocity of the wall. Symmetry with respect to the X-axis yields the boundary conditions

$$\left.\begin{aligned} \frac{\partial U}{\partial Y} &= 0 \\ V &= 0 \\ \frac{\partial W}{\partial Y} &= 0 \end{aligned}\right\} \text{along the } X\text{-axis boundary}$$

Two different types of boundary conditions are considered in the Z direction.

Case I: The axial pressure gradient is maintained constant, that is,

$$\frac{\partial P}{\partial Z} = \text{constant} \quad (2)$$

Condition (2) corresponds to flow from a constant pressure source, such as a standpipe, a tank of liquid pressurized by gas or a centrifugal pump in series with a large flow resistance.

Case II: The flux through the helix is maintained constant.

$$\int_{-1}^{1}\int_{-1}^{1} W_{rel}\, dX dY = \text{constant} \quad (3)$$

where

$$W_{rel} = W - W_0[1+(a/r)X]\sin \Omega T.$$

Condition (3) applies when there is a constant flow source, such as a gear pump driven at constant speed.

The flux through the helix is the net flow through a cross section fixed to the walls, that is, the integral of W_{rel}, the relative axial velocity of the fluid with respect to a coordinate system fixed to the walls. The flux through the helix is equal to the flux entering or leaving the stationary tubes affixed to the end of the helix.

METHOD OF SOLUTION

Equations (1a), (1b), and (1c) are solved using the numerical scheme developed in Part I. The important differences are in the choice of initial conditions and the test for convergence. The mesh is the same as employed in Part I.

The initial condition for the oscillating helix were the velocities in a straight pipe oscillating at the same amplitude, frequency and axial pressure gradient (in Case I) or throughput (in Case II). The equations describing flow through an oscillating straight tube are

$$\frac{\partial W}{\partial T} = \frac{\partial^2 W}{\partial X^2} + \frac{\partial^2 W}{\partial Y^2} - \frac{\partial P}{\partial Z} \quad (4)$$

$$W = W_0 \sin \Omega T \quad \text{on the wall boundary}$$

$$\frac{\partial W}{\partial Y} = 0 \quad \text{along} \quad X = 0$$

The above equations are solved using the same finite-difference technique used in solving Equations (1a), (1b), and (1c). The solution to the oscillating straight tube provided a close approximation to the axial velocity profile in the oscillating helix.

Equation (3), the integral constraint on the axial velocity in Case II, is satisfied by replacing the integral with a summation over all the mesh cells. The finite differenced equation for the axial velocity is substituted into the summation to obtain an equation for the axial pressure gradient. At the beginning of each time interval the axial pressure gradient at the succeeding time interval is calculated, and using this value the axial velocities are updated.

Convergence is assumed when the velocities at the beginning of consecutive oscillations differed by less than

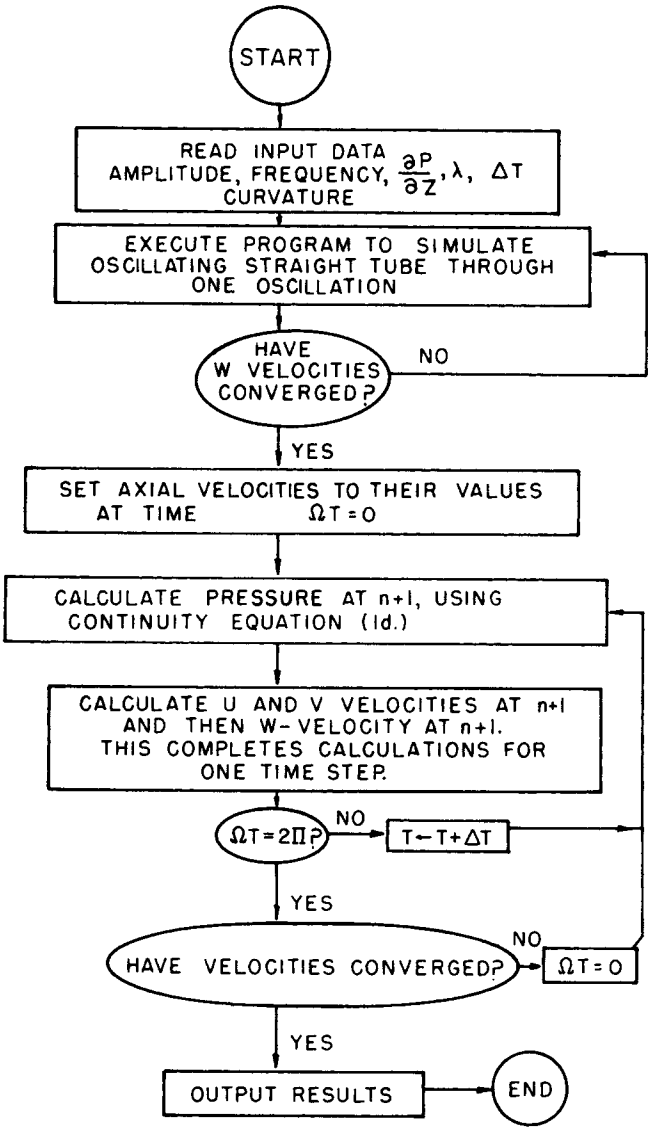

Fig. 2. Flow chart.

1%. The axial velocities for the straight oscillating pipe converged in less than ten oscillations. The solutions for the oscillating helix converged in three or fewer oscillations in all runs. The computing time required varied from three to four minutes per run on a UNIVAC 1108 computer.

Consistency of the solution was checked by repeating the calculation after halving the time step. About eighty steps per oscillation were required to maintain the accuracy of the solutions to 1% (percentages calculated with respect to the maximum value in the cross section).

A flow chart of the computer program is shown in Figure 2.

RESULTS

A summary of computed solutions is given in Table 1. In Runs 1 to 4 the axial pressure gradient was maintained constant (Boundary Condition I), and in Runs 5 to 7 the flow through the helix was maintained constant (Boundary Condition II). Axial velocity profiles and streamline contours for selected runs are shown in Figures 3 through 7. Appendix VI* gives more extended results. All runs

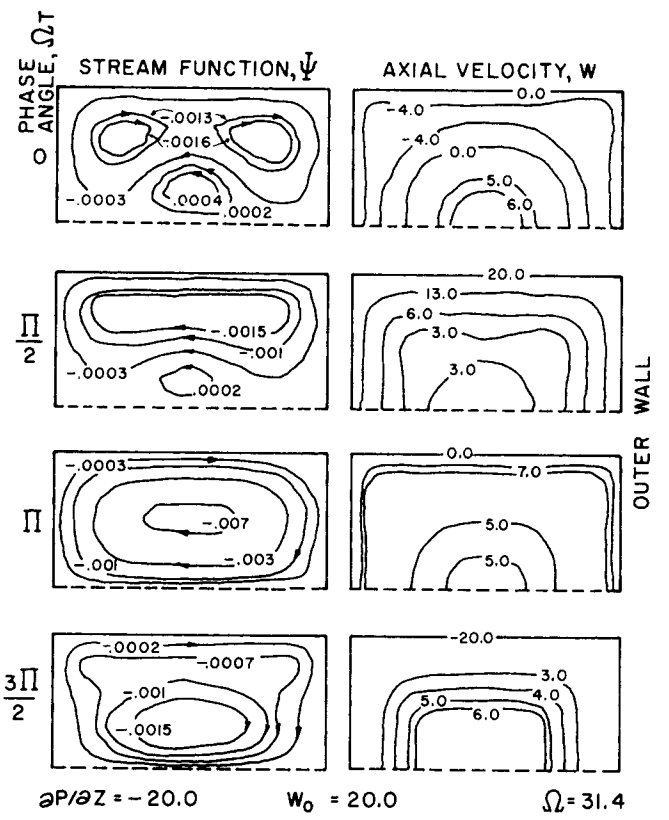

Fig. 3. Run 1, stream function and axial velocity.

TABLE 1. SUMMARY OF COMPUTED SOLUTIONS

Run No.	Figure No.‡	Boundary condition*	Amplitude, W_0	Axial pressure gradient, $\partial P/\partial Z$	Flux through helix, F
1	3	Case I	20.0	−20.0	11.001
2	4	Case I	20.0	0.0	0.000
3	5	Case I	20.0	−80.0	43.860
4	—	Case I	200.0	−80.0	44.610
5	6	Case II	20.0	Fig. VI-6	0.0
6	—	Case II	200.0	Fig. VI-9	10.0
7	7	Case II	20.0	Fig. 9	20.0

* Case I. Constant axial pressure gradient. See Equation (2). The flux through the helix varied with time. The value given is the time averaged flux.

* Case II. Constant flux. See Equation (3). The axial pressure gradient varies with time as shown in figures indicated.

$a/r = 0.02$ for all run numbers.

‡ Additional figures are contained in Appendix VI.

utilized the same dimensionless frequency of oscillation and curvature ratio of the helix. The computer program can be used for a wide range of curvature ratios; however, since the main objective was to investigate the interaction of flow and oscillation, the curvature ratio was not varied in this work. Similar considerations apply to the dimensionless frequency of oscillation (except that much higher frequencies would require a finer spatial mesh because the boundary layer becomes thinner as the frequency increases).

Runs 2, 4, 5, and 6 illustrate examples where the maximum wall velocity is greater than the velocity of flow, that is, the average velocity of the fluid flowing through the helix if it were stationary. The axial velocity of the fluid near the wall is greater than the velocity near the

* Appendix VI is contained in the supplement deposited as Document No. 02671 with the National Auxiliary Publications Service (NAPS), c/o Microfiche Publications, 440 Park Ave. So., N. Y., N. Y. 10016 and may be obtained for $1.50 for microfiche or $5.00 for photocopies.

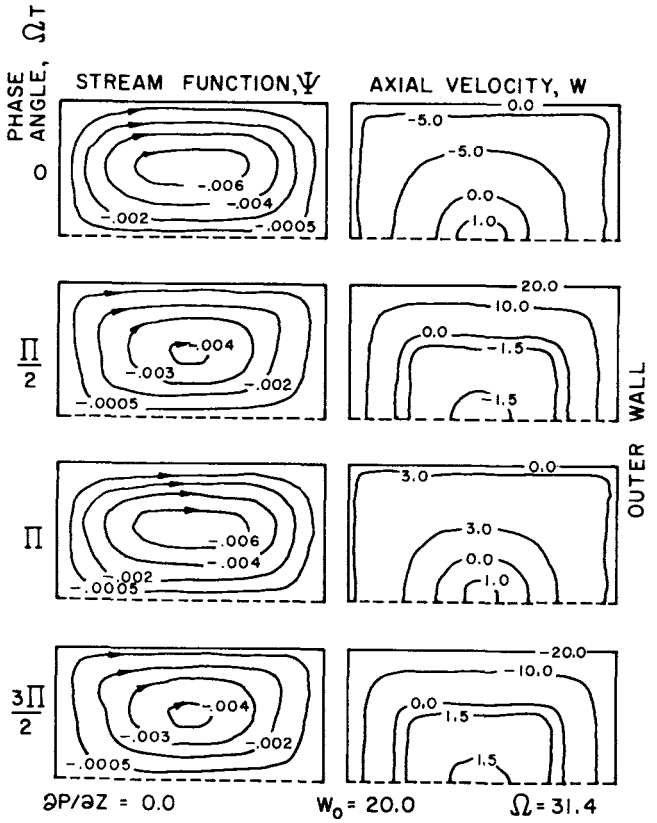

Fig. 4. Run 2, stream function and axial velocity.

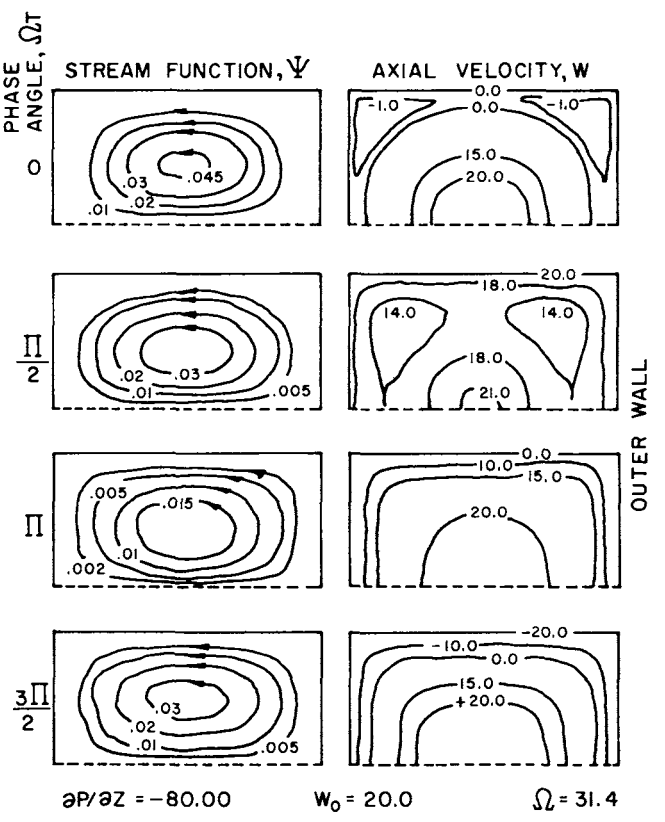

Fig. 5. Run 3, stream function and axial velocity.

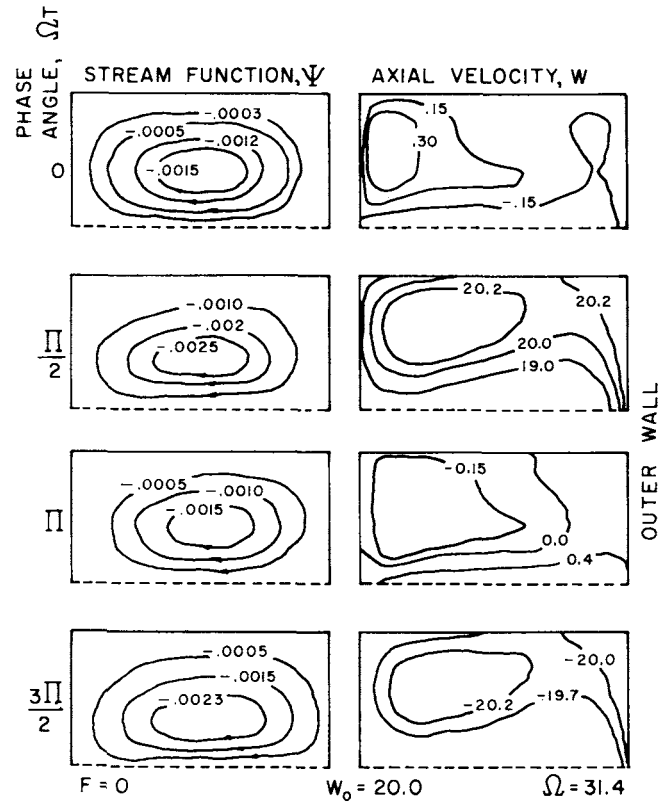

Fig. 6. Run 5, stream function and axial velocity.

center and the secondary velocities are opposite in direction to those observed in stationary helical coils. See Figures 4 and 6. The magnitude of the secondary flow strongly depends on the wall velocity.

In Run 3, the velocity of flow is greater than the wall velocity. The secondary velocity pattern is similar to that in stationary helices, but the magnitude of the secondary velocities is somewhat less and varies periodically with time due to the periodicity of the axial velocities near the wall.

Runs 1 and 7 illustrate cases where the velocity of flow and the maximum wall velocity are comparable. The point of maximum downstream velocity shifts from near the wall to near the center and back during the oscillation. The result is a complicated and changing secondary flow. In Run 7, the secondary flow completely reverses direction during the oscillation. In Run 1, up to six eddies are observed in the cross section due to the changing axial velocity profile. See Figure 3.

When Boundary Condition I is applied (Runs 1, 2, 3, and 4) the flux through the helix is approximately a sinusoidal function of time as illustrated by Figure 8 which gives the average axial velocity of the fluid, the average wall velocity and the average relative velocity of the fluid with respect to the wall for a typical run (Run 1). The average relative velocity of the fluid with respect to the wall is the flux through the helix divided by the area of the cross section of the helix.

The axial velocities in Case II are nearly constant throughout the cross section and approximately equal to the wall velocity. The fluid undergoes strong accelerations and decelerations in order to keep the flux through the helix constant. These accelerations require time-varying pressure gradients much larger than those required to maintain the same steady flux in a stationary helix. In Run 7, the axial pressure gradient varies from 6000 to −6000 during the oscillation whereas only an axial pressure gradient of about 20 is required to cause the same flux in a stationary helix. See Figure 9.

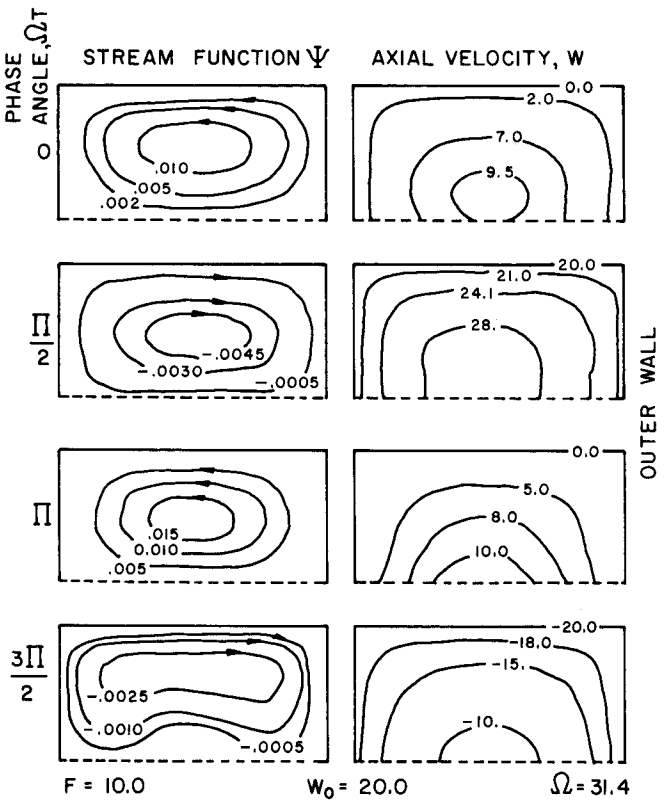

Fig. 7. Run 7, stream function and axial velocity.

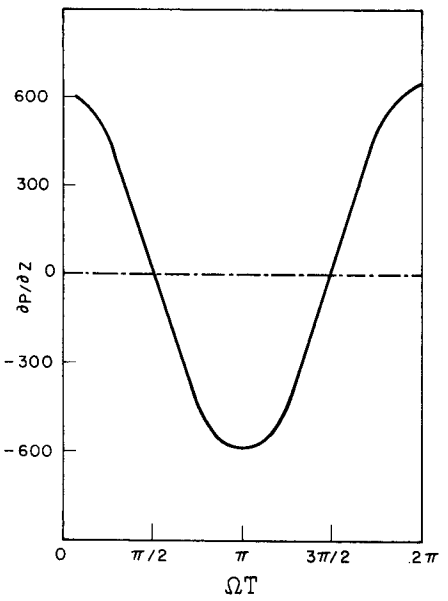

Fig. 9. Run 7, axial pressure gradient.

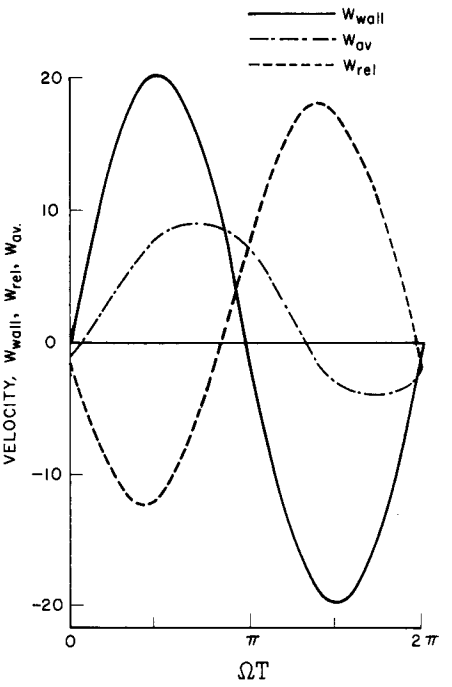

Fig. 8. Run 1, average axial velocities.

ACKNOWLEDGMENT

Financial support by the National Science Foundation, Grant GK 33818, is gratefully acknowledged.

NOTATION

a = half the width of the rectangular cross section in the X-direction

b = half the height of the rectangular cross section in the Y-direction, equal to a for square helices

F = flux through the helix $= 4\,\overline{W}_{rel}$

p = pressure

P = dimensionless pressure $= a^2p/\rho\nu^2$

r = radius of curvature of the helix

t = time

T = dimensionless time $= t\nu/a^2$

u = velocity in X-direction

U = dimensionless velocity in X-direction $= a\rho u/\mu$

v = velocity in Y-direction

V = dimensionless velocity in Y-direction

w = velocity in Z-direction measured in a stationary coordinate system. The coordinate system is shown in Part I of this work.

W = dimensionless velocity in Z-direction $= a\rho w/a$

W_{av} = dimensionless velocity in Z-direction averaged over the cross section $= \dfrac{1}{4}\displaystyle\int_{-1}^{1}\int_{-1}^{1} W\,dX\,dY$

W_0 = amplitude of wall velocity at $X = 0$, dimensionless

W_{rel} = relative velocity of fluid $= W - W_{wall}$

$\overline{W}_{rel}$ = relative velocity of fluid averaged over the cross section $= \dfrac{1}{4}\displaystyle\int_{-1}^{1}\int_{-1}^{1} W_{rel}\,dX\,dY = \dfrac{F}{4}$

W_{wall} = average wall velocity = wall velocity on the Y-axis $= W_0 \sin \Omega T$

x = dimensional coordinate in cross-sectional plane parallel to radius of curvature

X = dimensionless coordinate $= x/a$

y = dimensional coordinate in cross-sectional plane perpendicular to the radius of curvature

Y = dimensionless coordinate $= y/a\lambda$

z = curved spatial coordinate along tube centerline

Z = dimensionless coordinate $= z/a$

Greek Letters

λ = a parameter $= b/a = 1$ for square helices

μ = fluid viscosity

ν = fluid kinematic viscosity $= \mu/\rho$

ρ = fluid density

ψ = dimensionless stream function defined in Part I

ω = angular velocity

Ω = dimensionless angular velocity $= a^2\omega/\nu$

LITERATURE CITED

Bartlett, R. H., D. Kittredge, B. S. Noyes, Jr., R. H. Willard III, and P. A. Drinker, "Development of a Membrane Oxygenator: Overcoming Blood Diffusion Limitation," *J. Thoracic and Cardiovasc. Surgery*, **58**, 795 (1969).

Drinker, P. A., R. H. Bartlett, R. M. Bailer, and B. S. Noyes, Jr., "Augmentation of Membrane Gas Transfer by Induced Secondary Flows," *Surgery*, **66**, 775 (1969).

Fisher, J. C., U.S. Patents 2,898,858; 2,918,875; 2,936,713; 2,948,225; 2,951,450; 2,972,957; 3,080,822; 3,099,998 (1959-1963).

Moss, R. A., J. A. Benn, F. K. Ghadar, and P. A. Drinker, "Secondary Flow and Mass Transfer on an Oscillating Torus," *Adv. in Cardiology*, **6**, 40 (1971).

Manuscript received August 6, 1974; revision received and accepted March 14, 1975.

Oxygen Transfer in Fermentation

GEORGE T. TSAO and DOUGLAS D. LEE

Department of Chemical Engineering
Iowa State University
Ames, Iowa 50010

The rate of biological processes in aerobic fermentation and waste water treatment is often limited by the rate of dissolution of oxygen from air bubbles into the liquid. A clear understanding of interfacial resistance to oxygen transfer is thus of importance. An oxygen sensing microprobe was used to detect a stagnant film and a penetrable zone near an air-water interface contaminated with surfactants. The technique, when used in clean water, can also measure the frequency of surface renewal. A linear relationship was found between the square root of the renewal rate $s^{0.5}$ and the interfacial mass transfer coefficient k_L, which is predicted by the Danckwerts theory.

SCOPE

Mass transfer is an important phenomenon in all fermentations which always involve several heterogeneous phases. Even the simplest system contains at least two phases: discrete microbiological cells and a continuous aqueous solution of nutrients. In oxygen requiring processes of aerobic fermentation and waste water treatment, a third phase of air bubbles is often introduced. Gas-liquid contacting in microbiological systems is complicated by the fact that oxygen consuming microbiological cells are often absorbed on surfaces of gas bubbles, which creates a nonuniform distribution between the interfacial zone and the rest of the reaction mixture. Mass transfer theories for ordinary gas-liquid contacting do not seem to hold in biochemical and biological processes as observed and discussed by Tsao (1972), Lee and Tsao (1972, 1973), and Tsao, Mukerjee and Lee (1972).

Based upon his results on carbon dioxide absorption by an aqueous buffer in the presence of an enzyme, carbonic anhydrase, Tsao (1972) postulated an interfacial mass transfer model involving two zones: a stagnant film heavy with absorbed microbiological cells and absorbed surfactants and a renewable zone penetrable by liquid elements due to turbulence in the liquid bulk.

In this paper, an experimental examination of the two zones was made by using a microprobe sensor at the surface of a protein solution. The microprobe was used to measure not only the thickness of the stagnant film but also the frequency of renewal in the penetration zone. The experimental technique was also employed to investigate the interfacial phenomenon in a clean water system and provided some valuable experimental evidence of surface renewal.

CONCLUSIONS AND SIGNIFICANCE

An oxygen microprobe is an inert material coated, long needle with an exposed sensing tip of about 2 μ long and 1 μ wide, which detects the local oxygen concentration and sends signals to a picoammeter for readout and recording. In this work an oxygen microprobe was attached to a micromanipulator which allows three-dimensional movements of the sensing tip with increments of 5 μ. When a microprobe was placed near an air-water interface, typical signals on a recorder chart are shown in Figure 3. The experimental apparatus given in Figure 2 is essentially a stirred, gas absorption cell. When the water was stirred with the agitator at different speeds (revolutions per minute marked in Figure 3), the signals (reflecting local oxygen concentration) were found to fluctuate at different frequencies. Each of the abrupt changes on the recorder curves was interpreted to reflect a renewal of the surface with a liquid element freshly brought to the interfacial zone by the agitator. By counting the fluctuation frequency on the recorder charts, it was possible to obtain a linear correlation between k_L and $s^{0.5}$, shown in Figure 4. This linear correlation agrees with Danckwerts's surface renewal equation

$$k_L = (D\,s)^{0.5}$$

and provides a direct experimental support to the Danckwerts theory.

George T. Tsao is presently at the School of Chemical Engineering, Purdue University, West Lafayette, Indiana 47907.